Gravitational wave signatures of gauged baryon and lepton number

Jessica Bosch⬤, Zoraida Delgado⬤, Bartosz Fornal⬤, and Alejandra Leon⬤

Department of Chemistry and Physics, Barry University, Miami Shores, Florida 33161, USA

We demonstrate that novel types of gravitational wave signatures arise in theories with new gauge symmetries broken at high energy scales. For concreteness, we focus on models with gauged baryon number and lepton number, in which neutrino masses are generated via the type I seesaw mechanism, leptogenesis occurs through the decay of a heavy right-handed neutrino, and one of the new baryonic fields is a good dark matter candidate. Depending on the scalar content of the theory, the gravitational wave spectrum consists of contributions from cosmic strings, domain walls, and first order phase transitions. We show that a characteristic double-peaked signal from domain walls or a sharp domain wall peak over a flat cosmic string background may be generated. Those new signatures are within the reach of future experiments, such as Cosmic Explorer, Einstein Telescope, DECIGO, Big Bang Observer, and LISA.

I. INTRODUCTION

In the Standard Model [1–8], baryon number and lepton number are accidental global symmetries of the Lagrangian of an unknown origin. Although one expects both of those symmetries to be violated if grand unification is realized in nature [9,10], so far no sign of related processes, such as proton decay, have been observed in experiments [11], which excludes the minimal nonsupersymmetric version of those theories. If grand unification does not happen, then global baryon and lepton number may be a low-energy manifestation of some more fundamental gauge symmetries unbroken at high energy scales. Indeed, this line of reasoning is supported by the self-consistency of quantum theories of gravity, in which only gauge symmetries can be properly accommodated, unless unnatural conditions are introduced [12].

The first attempt to promote baryon and lepton number to the status of U(1) gauge symmetries dates back to the 1970s [13], and was followed by further theoretical efforts throughout the subsequent two decades [14–17]. However, the first phenomenologically viable model of this type was constructed only recently in [18], and later modified to avoid all current experimental bounds [19,20]. The idea of gauging baryon and lepton number was later successfully incorporated into a supersymmetric framework [21], theories unifying baryon number and color [22,23], and generalized to a non-Abelian gauged lepton number [24].

Models with gauged baryon and lepton numbers have very attractive features: they explain the stability of the proton, have a natural realization of the seesaw mechanism for neutrino masses, contain an attractive baryonic dark matter candidate [25–27], and can accommodate high scale leptogenesis [28]. Thus far, in all of the existing U(1) formulations of theories with gauged baryon and lepton number, each of the symmetries was broken by the vacuum expectation value of a single scalar. However, there is no reason to expect that the scalar sector is this minimal.

To this end, in this paper we investigate ways to probe the composition of high-scale symmetry breaking sectors, i.e., when at least one of the two sectors consists of more than one scalar breaking the symmetry. Although we focus on the class of theories with gauged baryon and lepton number, most of our analysis is general and can be applied to other theories with two broken U(1) gauge symmetries. Conventional particle physics experiments are not able to differentiate between the two scenarios, or even probe them at all if the symmetry breaking scale is high. Nevertheless, as we demonstrate below, gravitational wave detectors have opened up a completely new set of opportunities to probe such models.

A renaissance period for gravitational wave physics was initiated by the first direct detection of a gravitational wave signal coming from a black hole merger by the Laser Interferometer Gravitational Wave Observatory (LIGO) within the LIGO/Virgo collaboration [29]. By now, over one hundred of such events, involving also neutron stars, have been recorded. Those discoveries provide an ideal opportunity to test general relativity, but they are not directly related to particle physics. The gravitational waves that enable probing particle physics models, although not yet discovered, are expected to come in the

form of a stochastic gravitational wave background produced in the early Universe by phenomena such as inflation [30], first order phase transitions [31], domain walls [32], and cosmic strings [33,34]. Although for such signals to be detectable at LIGO the underlying particle physics models require a large fine-tuning of parameters, future gravitational wave experiments, such as the Laser Interferometer Space Antenna (LISA) [35], Cosmic Explorer [36], Einstein Telescope [37], DECIGO [38], and Big Bang Observer [39], will be sensitive to more generic scenarios.

The most model-independent stochastic gravitational wave background comes from cosmic strings, which are topological defects formed via the Kibble mechanism [40] upon a spontaneous breaking of a U(1) symmetry. They correspond to one-dimensional field configurations along the direction in which the symmetry remains unbroken. The dynamics of the produced cosmic string network provides a long-lasting source of gravitational radiation resulting in a mostly flat stochastic gravitational wave background, with its strength dependent only on the scale of the U(1) breaking. Cosmic string signatures have been considered in the context of grand unified theories [41,42], neutrino seesaw models [43–49], new physics at the high scale [50], as well as baryon and lepton number violation [51]. For a review of gravitational waves signatures of cosmic strings see [52], and for the constraints from LIGO/Virgo data see [53].

The other topological defects which can be produced in the early Universe are domain walls, created when a Z_2 symmetry is spontaneously broken. They are two-dimensional field configurations existing at the boundaries of regions corresponding to different vacua. In order for domain walls not to overclose the Universe, they need to annihilate away. This is possible when there exists a small energy density difference between the two vacua (the so-called potential bias). Domain wall annihilation leads to a stochastic gravitational wave background which is peaked at some frequency, but its strength and the peak frequency are, as in the case of cosmic strings, independent of the exact particle physics details of the model—the spectrum is determined by only two parameters: the scale of the symmetry breaking and the potential bias. Domain wall signatures have been considered in many theories beyond the Standard Model, including new electroweak scale physics [54–57], supersymmetry [58], axions [59–63], grand unification [64], models with left-right symmetry [65], baryon/lepton number violation [66], flavor symmetries [67], and leptogenesis [68]. The physics of domain walls and the expected gravitational wave spectrum are reviewed in [69]; the bounds on domain walls from LIGO/Virgo data can be found in [70].

The most model-dependent gravitational wave signatures arise from cosmological first order phase transitions. Those occur when the effective potential develops a new minimum with a lower energy density than the high-temperature one. If there exists a potential barrier between the two minima, the transition is first order and bubbles of true vacuum are being nucleated in various points in space. Such bubbles of true vacuum expand, eventually filling up the entire Universe. Gravitational waves are emitted from bubble collisions, turbulence, and sound shock waves in the primordial plasma generated by the violent expansion of the bubbles. The position of the gravitational wave peak is highly dependent on the temperature at which bubble nucleation occurs. First order phase transitions have been analyzed in a plethora of particle physics models, including, again, electroweak scale new physics [71–79], supersymmetry [80,81], axions [82–84], grand unification [85–87], baryon/lepton number violation [51,88]), neutrino seesaw models [89–92], new flavor physics [93,94], dark gauge groups [95–98], models with conformal invariance [99,100], and dark matter [101–107]. A comprehensive review of gravitational waves from first order phase transitions can be found in [108,109], while the most recent constraints from LIGO/Virgo data were derived in [110]. For recent progress on supercooled phase transitions, see [111–113].

In this work, we examine how gravitational wave signals from domain walls, cosmic strings, and phase transitions interplay with each other, producing novel features in the expected spectrum. The two new gravitational wave signatures which have not been considered in the literature so far are these:

(1) Two coexisting signals from domain wall annihilation, forming a characteristic sharp double-peak in the spectrum.

(2) Domain wall signal over a flat cosmic string contribution, leading to an unusually shaped peak.

Although we focus on a specific model, our results involving cosmic strings and domain walls, in particular signatures (1) and (2), are general, since they do not depend on the details of the model.

II. THE MODEL

The gravitational wave signatures we propose to search for, as will be discussed in Sec. VII, are anticipated in a large class of models with a multistep symmetry breaking pattern. In this paper, to provide a concrete realization of such scenarios, we focus on models with gauged baryon and lepton number, based on the gauge group

$$\mathrm{SU}(3)_c \times \mathrm{SU}(2)_L \times \mathrm{U}(1)_Y \times \mathrm{U}(1)_B \times \mathrm{U}(1)_L. \quad (1)$$

Below we describe the possible symmetry breaking sectors in such models and the new particles along with their masses.

A. Scalar sector

As mentioned in Sec. I, we consider extending the usual single-scalar symmetry breaking sector to include either

one or two scalars breaking each symmetry. The fields breaking the $U(1)_L$ symmetry come in the representation

$$\Phi_{Li} = (1, 1, 0, 0, 2), \tag{2}$$

with $i = 1$ or $i = 1, 2$, while the scalars breaking $U(1)_B$ are

$$\Phi_{Bj} = (1, 1, 0, 3, 3), \tag{3}$$

where $j = 1$ or $j = 1, 2$. Within this framework, there are four possible types of models:

Model (a) Two new scalar fields involved:
    Φ_{B1} breaks $U(1)_B$ and Φ_{L1} breaks $U(1)_L$.
Model (b) Three new scalar fields involved:
    Φ_{B1}, Φ_{B2} break $U(1)_B$ and Φ_{L1} breaks $U(1)_L$.
Model (c) Three new scalar fields involved:
    Φ_{B1} breaks $U(1)_B$ and Φ_{L1}, Φ_{L2} break $U(1)_L$.
Model (d) Four new scalar fields involved:
    Φ_{B1}, Φ_{B2} break $U(1)_B$ and Φ_{L1}, Φ_{L2} break $U(1)_L$.

We assume that the mixed terms involving scalars breaking different $U(1)$ gauge groups have negligible coefficients. This implies that, for a given $U(1)$, if only one scalar breaks the symmetry, then the scalar potential is

$$V(\Phi_1) = -m^2|\Phi_1|^2 + \lambda|\Phi_1|^4, \tag{4}$$

whereas if two scalars participate in symmetry breaking,

$$\begin{aligned}
V(\Phi_1, \Phi_2) = & -m_1^2|\Phi_1|^2 + \lambda_1|\Phi_1|^4 - m_2^2|\Phi_2|^2 + \lambda_2|\Phi_2|^4 \\
& + [(\lambda_4|\Phi_1|^2 + \lambda_5|\Phi_2|^2 + \lambda_6\Phi_1^*\Phi_2)\Phi_1^*\Phi_2 + \text{H.c.}] \\
& - (m_{12}^2\Phi_1^*\Phi_2 + \text{H.c.}) + \lambda_3|\Phi_1|^2|\Phi_2|^2,
\end{aligned} \tag{5}$$

where $\Phi_i = \Phi_{Li}$ or $\Phi_j = \Phi_{Bj}$. The scalars develop the following vacuum expectation values,

$$\langle \Phi_i \rangle = \frac{v_i}{\sqrt{2}}. \tag{6}$$

Whenever two scalars take part in the symmetry breaking, we define $v \equiv \sqrt{v_1^2 + v_2^2}$. This way one can collectively describe the $U(1)_B$ breaking scale as $v = v_B$, and the $U(1)_L$ breaking scale as $v = v_L$, independent of whether the vacuum expectation value comes from a single scalar or two scalars.

If the lepton number is broken at a higher scale than baryon number, the symmetry breaking pattern is

$$SU(3)_c \times SU(2)_L \times U(1)_Y \times U(1)_B \times U(1)_L$$
$$\downarrow \langle \Phi_{Li} \rangle \neq 0$$
$$SU(3)_c \times SU(2)_L \times U(1)_Y \times U(1)_B$$
$$\downarrow \langle \Phi_{Bj} \rangle \neq 0$$
$$SU(3)_c \times SU(2)_L \times U(1)_Y,$$

followed by the usual electroweak symmetry breaking by the Standard Model Higgs. We note that the order of $U(1)_B$ and $U(1)_L$ breaking may be reversed.

B. Fermion sector

To provide a concrete quantitative example, we consider the model with gauged $U(1)_B$ and $U(1)_L$ proposed in [20], which involves the minimal fermionic particle content for a theory with such a gauge group. It is straightforward to check that all gauge anomalies are canceled if the Standard Model quark fields Q_L^k, u_R^k, d_R^k and lepton fields l_L^k, e_R^k are augmented by

$$\nu_R^k = (1, 1, 0, 0, 1),$$
$$\Psi_L = \begin{pmatrix} \psi_L^+ \\ \psi_L^0 \end{pmatrix} = \left(1, 2, \frac{1}{2}, \frac{3}{2}, \frac{3}{2}\right),$$
$$\Psi_R = \begin{pmatrix} \psi_R^0 \\ \psi_R^- \end{pmatrix} = \left(1, 2, \frac{1}{2}, -\frac{3}{2}, -\frac{3}{2}\right),$$
$$\Sigma_L = \frac{1}{2}\begin{pmatrix} \sigma^0 & \sqrt{2}\,\sigma^+ \\ \sqrt{2}\,\sigma^- & -\sigma^0 \end{pmatrix} = \left(1, 3, 0, -\frac{3}{2}, -\frac{3}{2}\right),$$
$$\chi_L = \left(1, 1, 0, -\frac{3}{2}, -\frac{3}{2}\right), \tag{7}$$

where k is the family index. Among the fields above, ν_R^k are the right-handed neutrinos, whereas χ_L is a Majorana dark matter candidate discussed in Sec. III.

C. Particle masses

The scalars Φ_{Bj} and Φ_{Li} generate masses for the new fermions through the following Lagrangian terms,

$$\begin{aligned}
-\mathcal{L} \supset & \sum_j (Y_\Psi^j \bar{\Psi}_R \Psi_L \Phi_{Bj}^* + Y_\Sigma^j \text{Tr}(\Sigma_L^2)\Phi_{Bj} + Y_\chi^j \chi_L \chi_L \Phi_{Bj}) \\
& + y_\nu^k \bar{l}_L^k H \nu_R^k + \sum_i Y_\nu^{ik} \nu_R^k \nu_R^k \Phi_{Li} + \text{H.c.},
\end{aligned} \tag{8}$$

which provide vectorlike masses to the new fermions, as well as introduce a type I seesaw mechanism for the neutrinos. For example, assuming that the Yukawa couplings are $y_\nu^k \sim 1$ and $Y_\nu^{ik} \sim 10^{-2}$, the measured neutrino mass splittings are reproduced if $v_L \sim 10^5$ PeV. The mass matrices for the new fermions are provided in [20].

The spontaneous breaking of $U(1)_L$ and $U(1)_B$ leads to the appearance of vector gauge bosons Z_L and Z_B. Given the charges of the scalars breaking the two symmetries, the corresponding masses are

$$m_{Z_L} = 2g_L v_L, \qquad m_{Z_B} = 3g_B v_B, \tag{9}$$

where g_L and g_B are the $U(1)_L$ and $U(1)_B$ gauge couplings, respectively, whose values are free parameters.

III. DARK MATTER AND MATTER-ANTIMATTER ASYMMETRY

Apart from providing a natural framework accommodating a type I seesaw mechanism generating small neutrino masses via $U(1)_L$ breaking, the model also contains a phenomenologically viable dark matter candidate χ_L [20,26] and can account for the matter-antimatter asymmetry through leptogenesis [28]. We discuss the most relevant aspects of those highlights of the model below.

A. Dark matter

After $U(1)_B$ breaking, there remains a residual discrete Z_2 symmetry under which the new fermions transform as

$$\Psi_L \to -\Psi_L, \qquad \bar{\Psi}_R \to -\bar{\Psi}_R,$$
$$\Sigma \to -\Sigma, \qquad \chi_L \to -\chi_L. \qquad (10)$$

If χ_L is the lightest of the new fermions, then there is no decay channel available for it, thus it becomes a good candidate for particle dark matter.

It was argued in [25,27] that in models with gauged baryon and lepton number consistency with the dark matter relic abundance of $h^2\Omega_{DM} \approx 0.12$ [114] imposes an upper bound on the $U(1)_B$ breaking scale. In particular, if the dark matter annihilation happens via the resonant s-channel process

$$\chi_L\,\chi_L \to Z_B^* \to \bar{q}q, \qquad (11)$$

a dependence between the parameters v_B, Y_χ, and g_B arises, and the perturbativity requirement leads to $g_B v_B \lesssim 20$ TeV. This was the reason why in [51], where the gravitational wave signal from a model with gauged baryon and lepton number was considered, a low scale of $U(1)_B$ was imposed.

However, as was demonstrated in [26], in the model we are considering other dark matter annihilation channels remain unsuppressed, including the nonresonant t-channel process

$$\chi_L\,\chi_L \to \Phi_{Bj}\Phi_{Bj}, \qquad (12)$$

whose cross section can be sufficiently large to explain the dark matter relic density. Therefore, the arguments in [25,27] do not apply in our case, and the scale of $U(1)_B$ breaking can be high. Alternatively, the aforementioned bound on the $U(1)_B$ breaking scale can always be avoided by assuming nonthermal dark matter production.

B. Leptogenesis

There cannot exist any primordial baryon or lepton number asymmetry above the scales of $U(1)_B$ and $U(1)_L$ breaking. An excess of matter over antimatter can only arise once one of those two symmetries is broken. A natural setting to achieve this below the scale of $U(1)_L$

breaking is offered by high-scale leptogenesis (see [115] and references therein), in which a lepton number asymmetry is generated through the out-of-equilibrium decays of the lightest right-handed neutrino,

$$N_1 \to Hl_L. \qquad (13)$$

The CP asymmetry is introduced through the standard interference between the tree-level diagram for the process in Eq. (13) and the one-loop diagrams involving H, l_L, and the two heavier right-handed neutrinos N_2, N_3 in the loop.

The generated lepton asymmetry is calculated by solving the Boltzmann equations for the evolution of the lightest right-handed neutrino abundance $Y_{N_1} = n_{N_1}/s$ (where n_{N_1} is the N_1 particle density and s is the comoving entropy density) and the $B - L$ asymmetry Y_{B-L} [116],

$$\frac{dY_{N_1}}{dz} = -(D + S)(Y_{N_1} - Y_{N_1}^{eq}),$$
$$\frac{dY_{B-L}}{dz} = -\epsilon_1 D(Y_{N_1} - Y_{N_1}^{eq}) - WY_{B-L}, \qquad (14)$$

where $z = m_{N_1}/T$, the term D accounts for decays and inverse decays, S represents $\Delta L = 1$ scatterings, W describes the washout effects, and ϵ_1 is the CP asymmetry parameter. In our case, the Boltzmann equations are slightly different than in the standard leptogenesis scenario, since the right-handed neutrinos have an extra interaction with the Z_L gauge boson. Those equations were solved in [28], and the amount of the generated lepton asymmetry ΔL was determined for various values of model parameters.

The produced lepton asymmetry is then partially converted into a baryon asymmetry through the electroweak sphalerons. Above the scale of $U(1)_B$ breaking the sphaleron-induced interactions have the form

$$(QQQL)^3\bar{\Psi}_R\Psi_L\Sigma_L^4, \qquad (15)$$

and it was shown in [25] that if the breaking of $U(1)_B$ occurs close to the electroweak scale, then the final baryon asymmetry predicted by the model is given by

$$|\Delta B| = \frac{32}{99}|\Delta L|. \qquad (16)$$

This can explain the observed baryon-to-photon ratio [117]

$$\eta \approx 6 \times 10^{-10} \qquad (17)$$

if the scale of $U(1)_L$ breaking satisfies the relation

$$v_L \gtrsim 4000 \text{ PeV}. \qquad (18)$$

The requirement for such a high $U(1)_L$ symmetry breaking scale provides the desired setting accommodating the type I seesaw mechanism for the neutrinos.

IV. COSMIC STRING SPECTRUM

Spontaneous breaking of a U(1) gauge symmetry leads to the production of topological defects in the form of cosmic strings [40], which correspond to one-dimensional field configurations along the direction of the unbroken symmetry. The network of produced cosmic strings is described collectively by the string tension μ, equal to the energy stored in a string per unit length, and depends solely on the scale at which the U(1) gauge symmetry is broken [52,118],

$$G\mu = 2\pi \left(\frac{v}{M_{\text{Pl}}}\right)^2, \tag{19}$$

where $M_{\text{Pl}} = 1.22 \times 10^{13}$ PeV is the Planck mass, the gravitational constant $G = 6.7 \times 10^{-39}$ GeV^{-2}, and the winding number was taken to be one. The constraints from the cosmic microwave background measurements set an upper limit on the string tension of $G\mu \lesssim 10^{-7}$ [119], which corresponds to the following bound on the scale of symmetry breaking,

$$v \lesssim 1.5 \times 10^9 \text{ PeV}. \tag{20}$$

Through its dynamics, the cosmic string network provides a long-lasting source of gravitational radiation and leads to a stochastic gravitational wave background roughly constant across a wide range of frequencies.

A. Dynamics of cosmic strings

There are two main processes governing the behavior of a cosmic string network: formation of string loops and stretching due to the expansion of the Universe. The first of those contributions, the creation of string loops, happens when long strings intersect and intercommute. The newly created string loops oscillate and emit gravitational radiation, mainly from cusps and kinks propagating through the string loop, and from kink-kink collisions [120,121].

A competition between these two effects leads to the so-called scaling regime, in which there is a large number of string loops and a small number of Hubble-size strings [122–126]. There is a continuous flow of energy from long strings to string loops, and then to gravitational radiation through their decays. This gravitational radiation makes up a fixed fraction of the energy density of the Universe [127].

To describe this process quantitatively, we follow the steps outlined in [46,52]. We consider a string loop created at time t_0 with initial length $l(t_0) = \alpha t_0$, where α is a constant loop size parameter. The loop oscillates emitting gravitational waves with frequencies

$$\tilde{f} = \frac{2k}{l}, \tag{21}$$

where k is a positive integer. Rescaling this result by the scale factor $a(t)$, one obtains the currently observed frequency,

$$f = \frac{a(t_e)}{a(T)}\tilde{f}, \tag{22}$$

where t_e is the time of the emission and T is the time today. The spectrum of the emitted gravitational waves from a single oscillating string loop is given by [43,128]

$$P_{(k,n)} = \frac{\Gamma G\mu^2}{k^n} \left(\sum_{p=1}^{\infty} \frac{1}{p^n}\right)^{-1}, \tag{23}$$

where for the contribution from cusps $n = 4/3$, from kinks $n = 5/3$, and from kink-kink collisions $n = 2$, while the overall factor $\Gamma \simeq 50$ [129]. Due to the constant emission of gravitational radiation, the string loop shrinks and its length at the time of the gravitational wave emission is

$$l(t_e) = \alpha t_0 - \Gamma G\mu(t_e - t_0), \tag{24}$$

causing the loop to vanish after the time $\alpha t_0/(\Gamma G\mu)$.

The only model-dependent quantity describing the cosmic string network is the loop distribution function $F(l, t_0)$ for the created loops. Adopting the well-established model developed in [130–132], describing the string network just by the mean string velocity and the correlation length, leads in the scaling regime to the following formula,

$$F(l, t_0) = \frac{\sqrt{2}C_{\text{eff}}}{\alpha t_0^4} \delta(l - \alpha t_0), \tag{25}$$

where the constant C_{eff} depends on the era in the evolution of the Universe (for radiation $C_{\text{eff}} = 5.4$, whereas for the matter dominated era $C_{\text{eff}} = 0.39$ [46]).

B. Gravitational wave spectrum

The stochastic gravitational wave background generated by the dynamics of the cosmic string network is [46,52]

$$h^2\Omega_{\text{CS}}(f) = \frac{2h^2\mathcal{F}_\alpha}{\rho_c\alpha^2 f} \sum_{k,n} kP_{(k,n)} \int_{t_F}^{T} dt_e \frac{C_{\text{eff}}(t_{0k})}{t_{0k}^4}$$
$$\times \left(\frac{a(t_e)}{a(T)}\right)^5 \left(\frac{a(t_{0k})}{a(t_e)}\right)^3 \theta(t_{0k} - t_F), \tag{26}$$

where

$$t_{0k} = \frac{1}{\alpha}\left(\frac{2k}{f}\frac{a(t_e)}{a(T)} + \Gamma G\mu t_e\right). \tag{27}$$
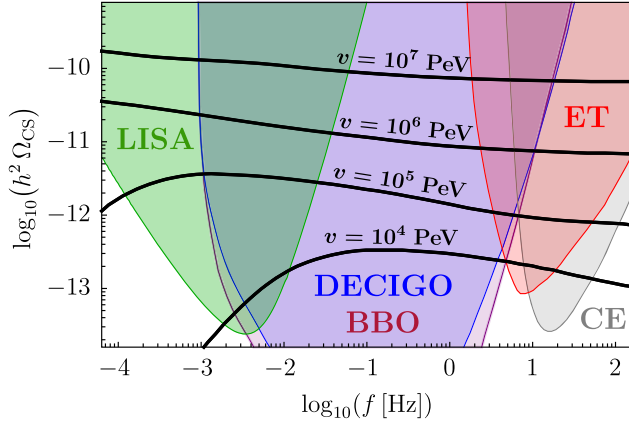
FIG. 1. Stochastic gravitational wave background from cosmic strings for four different symmetry breaking scales. Shaded regions correspond to the sensitivity of future gravitational wave detectors: LISA (green), DECIGO (blue), Big Bang Observer (purple), Einstein Telescope (red), and Cosmic Explorer (gray).

In Eqs. (26) and (27) the parameters are the following: $\mathcal{F}_\alpha$ is the fraction of the loops contributing to the gravitational wave signal, estimated to be $\mathcal{F}_\alpha \approx 0.1$ [128] since the majority of the energy is lost by long strings going into highly boosted smaller loops which provide only a sub-dominant contribution; ρ_c is the critical density of the Universe; the loop size parameter $\alpha = 0.1$ provides an accurate estimate of the loop size distribution [43,128]; t_F is the time at which the cosmic string network was formed, related to the density of the Universe at that time via $\sqrt{\rho(t_F)} = \mu$ [52], t_{0k} is the instance when the loop was produced, and $\theta(x)$ is the Heaviside step function. We assume that, as argued in [46,52], the largest contribution to the gravitational wave signal comes from the cusps.[1]

The resulting stochastic gravitational wave background is presented in Fig. 1 for four values of the symmetry breaking scale, in the range of frequencies relevant for the upcoming gravitational wave experiments, whose sensitivities are denoted by the colored regions. If $v \gtrsim 10^4$ PeV, then the signal can be seen by all the detectors: LISA [35], DECIGO [38], Big Bang Observer [39], Einstein Telescope [37], and Cosmic Explorer [36]. This is illustrated in more detail in Fig. 2, which shows the reach of each experiment in terms of the symmetry breaking scale leading to a cosmic string signal. The lower bound is detector specific, whereas the upper bound

---

[1]We note that there is an ongoing debate regarding the decay of cosmic strings. For example, it was argued in [133] that the leading contribution to the cosmic string gravitational wave signal arises from kink-kink collisions, whereas in [134] it was shown that the evolution of a string loop can be further altered due to the existence of localized excitations of the field theory string with a long lifetime. Such effects may lead to sizable modifications of the predicted gravitational wave spectrum. For a more general overview see [135].
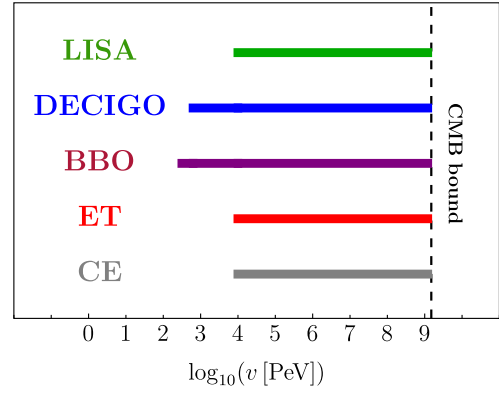

FIG. 2. Reach of future detectors in probing the scale of a U(1) symmetry breaking leading to the production of cosmic strings. The colors for each experiment correspond to those adopted in Fig. 1.

reflects the cosmic microwave background constraint in Eq. (20).

The cosmic string network will be produced if either $U(1)_B$ or $U(1)_L$ is spontaneously broken by a single scalar. Therefore, among the cases enumerated in Sec. II, the gravitational wave signals discussed here are relevant in case of model (a) for both baryon and lepton number breaking, model (b) only for lepton number breaking, and model (c) only for baryon number breaking.

V. DOMAIN WALL SPECTRUM

Another kind of topological defects, appearing when a U(1) symmetry is broken by two scalars, are domain walls. As in the case of SU(2) breaking discussed in [105], the effective potential $V(\phi_1, \phi_2, T)$, which at high temperature has just one vacuum at $(\phi_1, \phi_2) = (0,0)$, at lower temperature develops four vacua. They come in two pairs related via a gauge transformation, $\Phi_i \to e^{i\theta}\Phi_i$, and only two of them, say $\vec{\phi}_{\text{vac1}}$ and $\vec{\phi}_{\text{vac2}}$, correspond to disconnected manifolds, and thus are physically distinct. For a detailed discussion of the possible symmetry breaking patterns in models with two scalars, see [136–138]. After the phase transition takes place, patches of the Universe may end up in either one of the two vacua, leading to the creation of domain walls, i.e., two-dimensional field configurations on the boundaries of $\vec{\phi}_{\text{vac1}}$ and $\vec{\phi}_{\text{vac2}}$. In our analysis we will assume that the dynamics of the symmetry breaking leads precisely to such a scenario.

If the two vacua have identical energy densities, domain walls remain stable and considerably affect the evolution of the Universe, introducing unacceptably large density fluctuations [69]. Therefore, for a phenomenologically viable scenario, the Z_2 symmetry between the two vacua needs to be softly broken. It cannot be strongly broken, since then patches of the Universe would transition preferentially to

the lower energy density vacuum and domain walls would not form. In our case, the soft breaking of the Z_2 symmetry removing the degeneracy between the vacua is provided by the terms involving m_{12}^2, λ_4, and λ_5 in the Lagrangian in Eq. (5).

A. Dynamics of domain walls

The profile of the domain wall configuration $\vec{\phi}_{dw}(z)$ is the solution to the equation [56]

$$\frac{d^2\vec{\phi}_{dw}(z)}{dz^2} - \vec{\nabla}_\phi V_{\text{eff}}[\vec{\phi}_{dw}(z)] = 0, \qquad (28)$$

where the z axis was chosen to be perpendicular to the domain wall, and the boundary conditions are

$$\vec{\phi}_{dw}(-\infty) = \vec{\phi}_{\text{vac1}}, \qquad \vec{\phi}_{dw}(\infty) = \vec{\phi}_{\text{vac2}}. \qquad (29)$$

As mentioned earlier, there are only two parameters that describe the gravitational wave spectrum from domain walls. The first of them is the domain wall tension σ given by

$$\sigma = \int_{-\infty}^{\infty} dz \left[\frac{1}{2} \left(\frac{d\vec{\phi}_{dw}(z)}{dz} \right)^2 + V_{\text{eff}}[\vec{\phi}_{dw}(z)] \right]. \qquad (30)$$

In the model we are considering, to a good approximation

$$\sigma \sim v^3. \qquad (31)$$

The other parameter is the potential bias $\Delta\rho$, i.e., the energy density difference between the vacua, in our case equal to

$$\Delta\rho = \left(m_{12}^2 + \frac{1}{2}\lambda_4 v_1^2 + \frac{1}{2}\lambda_5 v_2^2 \right) v_1 v_2. \qquad (32)$$

The created domain walls are unstable and undergo annihilation, emitting gravitational radiation, provided that [69]

$$\Delta\rho \gtrsim \left(\frac{\sigma}{M_{\text{Pl}}} \right)^2. \qquad (33)$$

If in Eq. (32) the term involving m_{12}^2 is the dominant one, then Eq. (33) takes the form $m_{12} \gtrsim v^2/M_{\text{Pl}}$. For example, if the symmetry breaking scale is $v \sim 10^3$ PeV, this implies $m_{12} \gtrsim 100$ MeV. An independent constraint arises from the necessity of domain wall annihilation happening before big bang nucleosynthesis, so the ratios of the produced elements are not altered, but the bound in Eq. (33) remains stronger.

B. Gravitational wave spectrum

Domain wall annihilation leads to a stochastic gravitational wave background given by [58,69][2]

$$h^2\Omega_{\text{DW}}(f) \approx 7.1 \times 10^{-33} \left(\frac{\sigma}{\text{PeV}^3} \right)^4 \left(\frac{\text{TeV}^4}{\Delta\rho} \right)^2 \left(\frac{100}{g_*} \right)^{\frac{1}{3}}$$
$$\times \left[\left(\frac{f}{f_d} \right)^3 \theta(f_d - f) + \left(\frac{f_d}{f} \right) \theta(f - f_d) \right], \qquad (34)$$

where for the area parameter we used $\mathcal{A} = 0.8$ and for the efficiency parameter we adopted the value $\tilde{\epsilon}_{\text{gw}} = 0.7$ [139], θ denotes the step function, and the peak frequency f_d is

$$f_d \approx (0.14 \text{ Hz}) \sqrt{\frac{\text{PeV}^3}{\sigma} \frac{\Delta\rho}{\text{TeV}^4}}. \qquad (35)$$

The slope of the signal falls $\sim f^3$ to the left of the peak when moving toward lower frequencies, and falls like f^{-1} to the right of the peak when moving toward higher frequencies. The cosmic microwave background constraint on the strength of the signal at the peak is $h^2\Omega(f) < 2.9 \times 10^{-7}$ [142], which translates to the following condition on the parameters,

$$\frac{\sigma}{\sqrt{\Delta\rho}} \lesssim 2.5 \times 10^{12} \text{ PeV}, \qquad (36)$$

which is stronger than the bound imposed by Eq. (33).

Several examples of gravitational wave spectra from domain wall annihilation, plotted using Eq. (34), are shown in Fig. 3 for representative values of the parameters v and $\Delta\rho$. The reach of the upcoming gravitational wave detectors is also shown, including LISA, Big Bang Observer, DECIGO, Einstein Telescope, and Cosmic Explorer. A more detailed look at their sensitivity is provided by Fig. 4, which shows the full parameter space that can be probed by those experiments. The lower bound on the domain wall parameter $\Delta\rho$ is a reflection of the cosmic microwave background constraint from Eq. (36). The parameter $\Delta\rho$ depends in general on all three fundamental Lagrangian parameters m_{12}, λ_4, and λ_5 through the relation in Eq. (32). Under the assumption that the term involving m_{12} is dominant, the experimental sensitivity plot in the plane (v, m_{12}) would be the same as in Fig. 4 of [66].

---

[2]We assume the shape of the domain wall spectrum suggested by the results of the numerical simulations presented in [139]. However, we note that due to the existing uncertainties in numerical determination of the corresponding parameters, other spectral shapes are also considered in the literature (see, e.g., [140,141]).
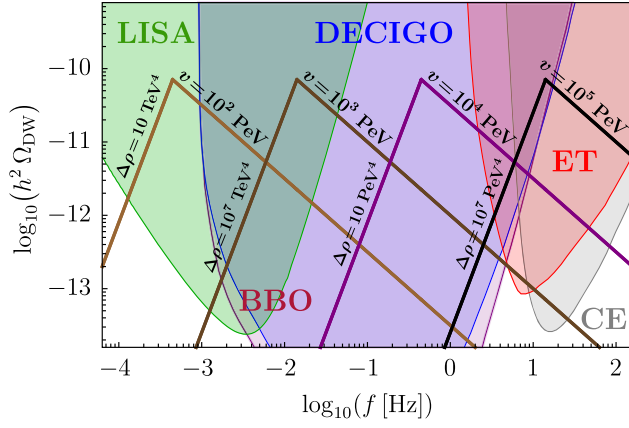
FIG. 3. Stochastic gravitational wave background from domain walls for various symmetry breaking scales. Shaded regions correspond to the sensitivity of future gravitational wave detectors, as in Fig. 1.
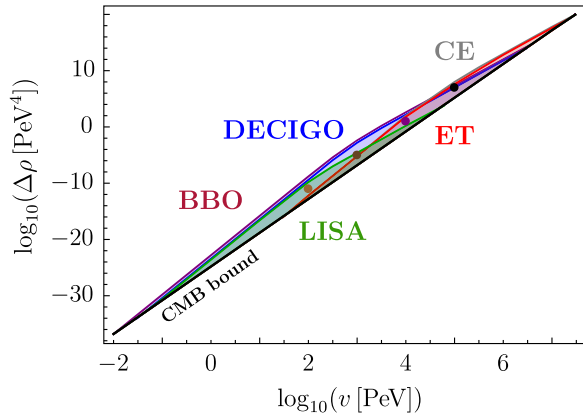

FIG. 4. Regions of parameter space $(v, \Delta\rho)$ for which the signal-to-noise ratio of the gravitational wave signal generated by domain wall annihilation is greater than five upon one year of data taking by various experiments. The choice of colors matches that in Fig. 3, including the color of the dots which correspond to the four curves.

VI. FIRST ORDER PHASE TRANSITION SPECTRUM

Perhaps the most anticipated stochastic gravitational wave signal to be discovered is the one generated by a first order phase transition in the early Universe, predicted in a large class of theories beyond the Standard Model. Such a signature in the case of $U(1)_B$ breaking has been considered in [51], but in this work we adopt a different assumption for the Yukawa couplings and keep our analysis more general, so that it can be applied to both gauged $U(1)_B$ and gauged $U(1)_L$. A first order phase transition can occur either when the symmetry breaking sector consists of a single scalar, or contains multiple scalars. Since the

generalization is straightforward, we concentrate on the case with a single scalar.

A. Effective potential

The effective potential for the background field ϕ consists of the tree-level part, the one-loop Coleman-Weinberg zero temperature correction, and the finite temperature contribution. Upon imposing the condition that the minimum of the zero temperature potential and the mass of ϕ remain at their tree-level values (i.e., the cutoff regularization scheme), the effective potential is given by

$$
\begin{aligned}
V_{\text{eff}}(\phi, T) \\
= -\frac{1}{2}\lambda v^2 \phi^2 + \frac{1}{4}\lambda\phi^4 \\
+ \sum_i \frac{n_i m_i^2(\phi)}{64\pi^2}\left\{ m_i^2(\phi)\left[\log\left(\frac{m_i^2(\phi)}{m_i^2(v)}\right) - \frac{3}{2}\right] + 2m_i^2(v)\right\} \\
+ \frac{T^4}{2\pi^2}\sum_i n_i \int_0^\infty dx\, x^2 \log\left(1 \mp e^{-\sqrt{m_i^2(\phi)/T^2 + x^2}}\right) \\
+ \frac{T}{12\pi}\sum_j n_j'\{m_j^3(\phi) - [m_j^2(\phi) + \Pi_j(T)]^{\frac{3}{2}}\}.
\end{aligned}
\tag{37}
$$

In the expression above the sums are over all particles charged under the $U(1)$ including the Goldstone bosons χ_{GB}, $m_i(\phi)$ are the field-dependent masses, n_i is the number of degrees of freedom for a given particle ($n_{Z'} = 3$, $n_\phi = 1$, $n_{\chi_{\text{GB}}} = 1$), n_j' is similar but includes only scalars and longitudinal components of vector bosons ($n_{Z'}' = 1$, $n_\phi' = 1$, $n_{\chi_{\text{GB}}}' = 1$), and for the Goldstones one needs to replace $m_{\chi_{\text{GB}}}(v) \to m_\phi(v)$. We will assume that all new Yukawa couplings are small, so that the only relevant field-dependent masses are

$$
m_{Z'}(\phi) = xg\phi, \qquad m_\phi(\phi) = \sqrt{\lambda(3\phi^2 - v^2)},
$$
$$
m_{\chi_{\text{GB}}}(\phi) = \sqrt{\lambda(\phi^2 - v^2)}.
\tag{38}
$$

In the limit $\lambda \ll g$, the thermal masses are

$$
\Pi_{Z'}(T) = \frac{1}{3}\left(x^2 + \frac{9}{2}\right)g^2 T^2,
$$
$$
\Pi_\phi(T) = \Pi_{\chi_{\text{GB}}}(T) = \frac{1}{4}x^2 g^2 T^2,
\tag{39}
$$

where for gauged baryon number $g = g_B$ and $x = 3$, while for gauged lepton number $g = g_L$ and $x = 2$.

For a range of λ and g values the effective potential develops a vacuum at $\phi \neq 0$ (true vacuum) with a lower energy density than the high temperature vacuum at $\phi = 0$ (false vacuum), separated by a potential bump, which are precisely the conditions needed for a first order phase
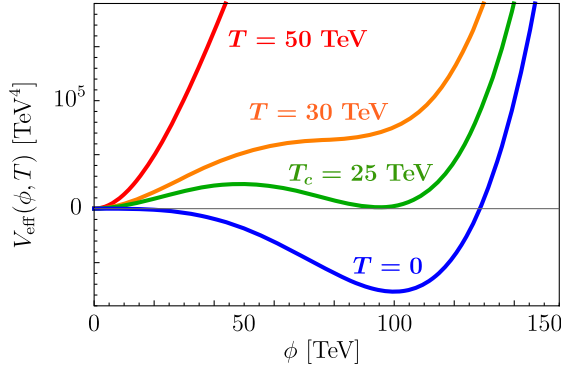
FIG. 5. The effective potential of the model, $V_{\text{eff}}(\phi_B, T)$, plotted for $v_B = 100$ TeV, $g_B = 0.25$, $\lambda_B = 0.006$, and several temperatures.

transition to take place.[3] The changing shape of the effective potential is shown in Fig. 5 for a particular choice of parameters, in the case of gauged baryon number.

B. Dynamics of the phase transition

A first order phase transition from the false vacuum to the true vacuum of a given patch of the Universe corresponds to the nucleation of a bubble which then starts expanding. This process is initiated at the nucleation temperature T_*, which is determined from the condition that the bubble nucleation rate [145] becomes comparable with the Hubble expansion,

$$\left(\frac{S(T_*)}{2\pi T_*}\right)^{3/2} T_*^4 e^{-S(T_*)/T_*} \approx H(T_*)^4, \quad (40)$$

where $S(T)$ is the Euclidean action given by

$$S(T) = \int d^3 r \left[\frac{1}{2}\left(\frac{d\phi_b}{dr}\right)^2 + V_{\text{eff}}(\phi_b, T)\right], \quad (41)$$

with ϕ_b being the solution of the bubble equation,

$$\frac{d^2\phi}{dr^2} + \frac{2}{r}\frac{d\phi}{dr} - \frac{dV_{\text{eff}}(\phi, T)}{d\phi} = 0, \quad (42)$$

subject to the boundary conditions

$$\left.\frac{d\phi}{dr}\right|_{r=0} = 0, \qquad \phi(\infty) = \phi_{\text{false}}. \quad (43)$$

Since $H(T) \approx (T^2/M_{\text{Pl}})\sqrt{4\pi^3 g_*/45}$, Eq. (40) becomes

---

[3]The shape of the effective potential depends on the regularization scheme, gauge, renormalization scale, and treatment of the Goldstone catastrophe and Daisy diagrams. Various choices may lead to vastly different values of the first order phase transition parameters, impacting the predictions for the expected gravitational wave signal [143,144].

$$\frac{S(T_*)}{T_*} \approx 4\log\left(\frac{M_{\text{Pl}}}{T_*}\right) - \log\left[\left(\frac{4\pi^3 g_*}{45}\right)^2\left(\frac{2\pi T_*}{S(T_*)}\right)^{\frac{3}{2}}\right]. \quad (44)$$

The phase transition parameters relevant for determining the gravitational wave signal are the bubble wall velocity v_w, the nucleation temperature T_*, the phase transition strength α, and its duration $1/\tilde{\beta}$. In our analysis we assume $v_w = c$, but other choices are also possible [146,147]. The other three parameters, T_*, α, and $\tilde{\beta}$, are determined from the behavior of the effective potential with changing temperature. As such, those parameters encode information about the details of the particle physics model considered.

The phase transition strength is calculated as the ratio of the energy density difference between the false and true vacuum, and that of radiation, both taken at nucleation temperature,

$$\alpha = \frac{\rho_{\text{vac}}(T_*)}{\rho_{\text{rad}}(T_*)}. \quad (45)$$

Those two quantities are obtained from the relations

$$\begin{aligned}\rho_{\text{vac}}(T) = &\, V_{\text{eff}}(\phi_{\text{false}}, T) - V_{\text{eff}}(\phi_{\text{true}}, T)\\&- T\frac{\partial}{\partial T}[V_{\text{eff}}(\phi_{\text{false}}, T) - V_{\text{eff}}(\phi_{\text{true}}, T)],\end{aligned}$$

$$\rho_{\text{rad}}(T) = \frac{\pi^2}{30}g_* T^4, \quad (46)$$

where g_* is the number of degrees of freedom active when the bubbles are nucleated. The parameter $\tilde{\beta}$, related to the timescale of the phase transition, is determined via

$$\tilde{\beta} = T_*\frac{d}{dT}\left(\frac{S(T)}{T}\right)\bigg|_{T=T_*}. \quad (47)$$

C. Gravitational wave spectrum

The dynamics of the nucleated bubbles generates gravitational waves through sound shock waves in the early Universe plasma, bubble collisions, and magnetohydrodynamic turbulence. The expected contribution of each of those processes to the stochastic gravitational wave background was determined through numerical simulations, and the corresponding empirical formulas were derived. The resulting gravitational wave signal is the sum of the three contributions,

$$h^2\Omega_{\text{PT}}(f) = h^2\Omega_s(f) + h^2\Omega_c(f) + h^2\Omega_t(f). \quad (48)$$

The expected signal from sound waves is [147,148]

$$\begin{aligned}h^2\Omega_s(f) \approx &\, \frac{1.9 \times 10^{-5}}{\tilde{\beta}}\left(\frac{\kappa_s\alpha}{\alpha+1}\right)^2\left(\frac{100}{g_*}\right)^{\frac{1}{3}}\Upsilon\\&\times \frac{(f/f_s)^3}{[1 + 0.75(f/f_s)^2]^{7/2}},\end{aligned} \quad (49)$$

where f_s is the peak frequency, κ_s is the fraction of the latent heat transformed into the bulk motion of the plasma [146], and Υ is the suppression factor [149,150],

$$f_s = (0.19 \text{ Hz}) \left(\frac{T_*}{1 \text{ PeV}} \right) \left(\frac{g_*}{100} \right)^{\frac{1}{6}} \tilde{\beta},$$

$$\kappa_s = \frac{\alpha}{0.73 + 0.083\sqrt{\alpha} + \alpha},$$

$$\Upsilon = 1 - \frac{1}{\left[1 + \frac{8\pi^{\frac{1}{3}}}{\tilde{\beta}} \left(\frac{\alpha+1}{3\kappa_s \alpha} \right)^{\frac{1}{2}} \right]^{\frac{1}{2}}}. \tag{50}$$

The signal from bubble wall collisions is [31,147,151] (see [152] for recent updates)

$$h^2 \Omega_c(f) \approx \frac{4.9 \times 10^{-6}}{\tilde{\beta}^2} \left(\frac{\kappa_c \alpha}{\alpha+1} \right)^2 \left(\frac{100}{g_*} \right)^{\frac{1}{3}}$$

$$\times \frac{(f/f_c)^{2.8}}{1 + 2.8(f/f_c)^{3.8}}, \tag{51}$$

where now f_c is the peak frequency and κ_c is the fraction of the latent heat deposited into the bubble front [153],

$$f_c = (0.037 \text{ Hz}) \left(\frac{T_*}{1 \text{ PeV}} \right) \left(\frac{g_*}{100} \right)^{\frac{1}{6}} \tilde{\beta},$$

$$\kappa_c = \frac{\frac{4}{27}\sqrt{\frac{3}{2}\alpha} + 0.72\alpha}{1 + 0.72\alpha}. \tag{52}$$

The final contribution is provided by turbulence [154,155]

$$h^2 \Omega_t(f) \approx \frac{3.4 \times 10^{-4}}{\tilde{\beta}} \left(\frac{\epsilon \kappa_s \alpha}{\alpha+1} \right)^{\frac{3}{2}} \left(\frac{100}{g_*} \right)^{\frac{1}{3}}$$

$$\times \frac{(f/f_t)^3}{(1 + 8\pi f/f_*)(1 + f/f_t)^{11/3}}, \tag{53}$$

where $\epsilon = 0.05$ [147], while the peak frequency f_t and the parameter f_* are

$$f_t = (0.27 \text{ Hz}) \left(\frac{g_*}{100} \right)^{\frac{1}{6}} \left(\frac{T_*}{1 \text{ PeV}} \right) \tilde{\beta},$$

$$f_* = (0.17 \text{ Hz}) \left(\frac{g_*}{100} \right)^{\frac{1}{6}} \left(\frac{T_*}{1 \text{ PeV}} \right). \tag{54}$$

The resulting gravitational wave signals from the first order phase transition triggered by $U(1)_B$ breaking are shown in Fig. 6 for several symmetry breaking scales: 10 TeV (light brown curve), 100 TeV (brown curve), 1 PeV (purple curve), and 10 PeV (black curve). The gauge coupling was assumed to be $g_B = 0.25$, and the quartic coupling was chosen to be $\lambda_B = 0.006$. Spectra with peaks at larger frequencies correspond to higher symmetry breaking scales.
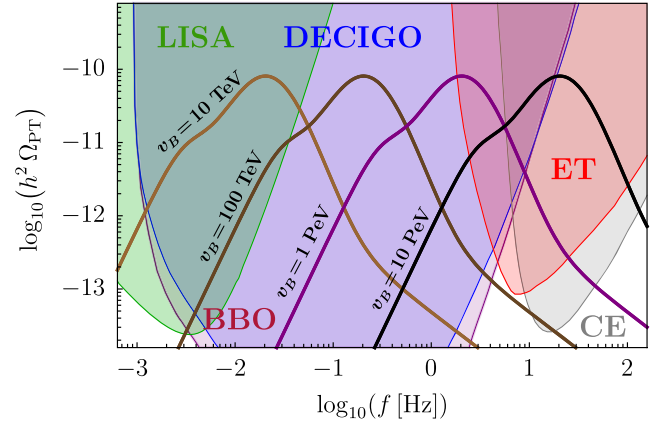

FIG. 6. Stochastic gravitational wave background from first order phase transitions triggered by $U(1)_B$ breaking assuming the model parameters $g_B = 0.25$ and $\lambda_B = 0.006$, for several choices of the symmetry breaking scale. The shaded regions correspond to the sensitivity of future gravitational wave detectors, as in Fig. 1.

The effect of the suppression factor Υ reducing the sound wave contribution in Eq. (49) is that the bubble collision and turbulence components become distinguishable in the spectrum. Although the main peak is still due to sound waves, the slope at lower frequencies is dominated by bubble collisions, whereas for higher frequencies the turbulence contribution visibly changes the slope of the curve. Without the suppression factor, the spectrum would be determined, to a good approximation, just by the sound wave component in the region relevant for future detectors.[4]

Depending on the Lagrangian parameters, the signal may be detectable in upcoming gravitational wave experiments: LISA, DECIGO, Big Bang Observer, Einstein Telescope, and Cosmic Explorer. To study this more quantitatively, in Fig. 7 we show part of the (g_B, λ_B) parameter space for which the signal can be detected in each experiment when $v_B = 1$ PeV. Specifically, the upper boundary for each detector corresponds to a signal-to-noise ratio of five upon a single year of data taking, while the lower boundary arises when either $S(T)/T$ is too large to satisfy Eq. (44) or the new vacuum has an energy density larger than that of the high temperature vacuum.

As mentioned earlier, our analysis of the first order phase transition signal from $U(1)_B$ breaking differs from the one in [51] in several aspects. The fermionic particle content in Eq. (7) is different, and we chose the corresponding Yukawa couplings to be small, which is a more minimal

---

[4]Predictions for the parameters of first order phase transitions are altered if one considers deflagrations or detonations [156], as well as sound-shell collisions during bubble percolations [157]. It was also shown that a double broken power law approximation [158] with one extra parameter leads to a significant improvement in fitting to the predictions of the sound shell model compared to the single broken power law [159].
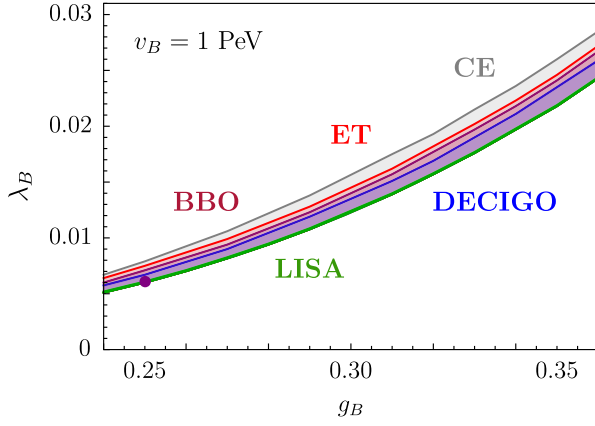
FIG. 7. Regions of parameter space (g_B, λ_B) assuming $v_B = 1$ PeV where the gravitational wave signal from a first order phase transition has a signal-to-noise ratio greater than five upon one year of data taking in various experiments. The choice of colors matches that in Fig. 6, and the dot corresponds to the purple curve.
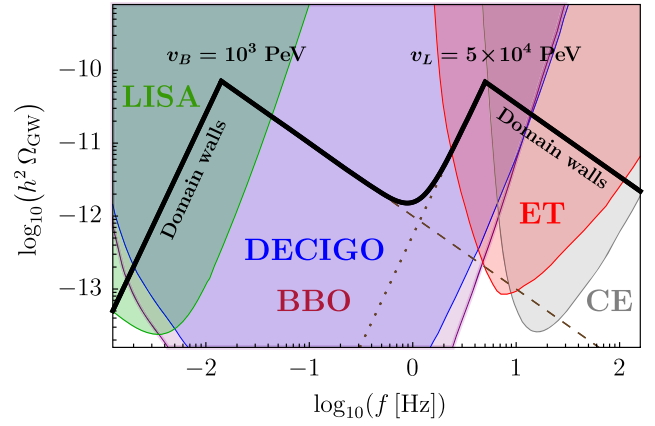

FIG. 8. First novel gravitational wave signature of the model consisting of a double domain wall peak, realized when each of the U(1) symmetries is broken by two scalars—model (d).

scenario than $Y = 0.6$ in [51]. Our analysis is also applicable to U(1)$_L$ breaking, since we calculate the thermal masses in the general case—this result will be used in Sec. VII. Finally, when determining the gravitational wave signal we included the effect of bubble collisions, which was not considered in [51], but which increases the reach of upcoming detectors due to the enhancement of the signal in the lower frequency region.

VII. GRAVITATIONAL WAVE SIGNATURES

In this section we demonstrate the diversity of gravitational wave signatures expected within the framework of the model, searchable in near-future experiments. The cases enumerated in Sec. II, corresponding to the possible structures of the scalar sectors, give rise to the coexistence in the spectrum of the following gravitational wave signals from first order phase transitions (PT), cosmic strings (CS), and domain walls (DW):

    (a) $(\mathrm{PT} + \mathrm{PT}), (\mathrm{PT} + \mathrm{CS}), (\mathrm{CS} + \mathrm{CS})$;
(b, c) $(\mathrm{PT}+\mathrm{PT}), (\mathrm{PT}+\mathrm{CS}), (\mathrm{PT}+\mathrm{DW}), (\mathrm{CS}+\mathrm{DW})$; and
    (d) $(\mathrm{PT} + \mathrm{PT}), (\mathrm{PT} + \mathrm{DW}), (\mathrm{DW} + \mathrm{DW})$.

We discuss below explicit examples of how those signatures are realized in our model. Two of them, $(\mathrm{DW} + \mathrm{DW})$ and $(\mathrm{CS} + \mathrm{DW})$ have not been considered in the literature before, whereas $(\mathrm{PT} + \mathrm{CS}), (\mathrm{PT} + \mathrm{PT})$, and $(\mathrm{PT} + \mathrm{DW})$ have been already proposed. The case $(\mathrm{CS} + \mathrm{CS})$ does not give rise to any new features, since the signal is dominated by the cosmic string contribution from the higher symmetry breaking due to the flatness of the cosmic string spectrum.

A. Domain walls + domain walls

A new gravitational wave signature arises when each of the two U(1) symmetries is broken by two scalars, leading

to the production of domain walls at two different energy scales during the evolution of the Universe. The signal consists of two sharp domain wall peaks. The slope on the left side of each peak depends on the frequency like $\sim f^3$, whereas the slope on the right side of the peak falls like $\sim 1/f$. There is a nontrivial structure created between the two peaks, which can be used to distinguish this type of signal from others. If the two symmetry breaking scales are high, then this signature can be searched for in all the upcoming gravitational wave experiments we considered: LISA, DECIGO, Big Bang Observer, Einstein Telescope, and Cosmic Explorer. A realization of this scenario in our model is shown in Fig. 8, where the parameters for the U(1)$_B$ breaking were chosen to be $v_B = 10^3$ PeV and $\Delta\rho = 10^{-5}$ PeV^4, whereas for the U(1)$_L$ breaking they are $v_L = 5 \times 10^4$ PeV and $\Delta\rho = 1.6 \times 10^5$ PeV^4.

B. Cosmic strings + domain walls

Another gravitational wave signature, not considered in the literature before, is realized when one of the U(1) symmetries is broken by one scalar, leading to cosmic string production, whereas the other U(1) is broken by two scalars, resulting in domain wall creation. If the two symmetry breaking scales are high, then their contributions may overlap and produce a very unusual domain wall peak over the cosmic string background. An example is shown in Fig. 9, where the symmetry breaking scale for U(1)$_L$ was chosen to be $v_L = 10^6$ PeV, whereas the parameters for U(1)$_B$ breaking are $v_B = 8 \times 10^3$ PeV and $\Delta\rho = 2$ PeV^4. For this particular selection of parameters, Big Bang Observer and DECIGO can probe the peak area, but for lower U(1)$_B$ breaking scales this structure is accessible to LISA, whereas higher symmetry breaking scales would make it detectable by Einstein Telescope and Cosmic Explorer.
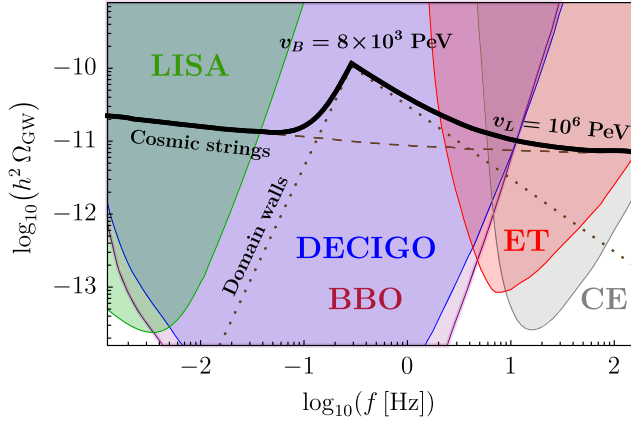
FIG. 9. Second novel gravitational wave signature consisting of a domain wall peak over a cosmic string background, realized when one U(1) symmetry is broken by one scalar and the other U(1) is broken by two scalars—models (b) and (c).

C. Phase transition + cosmic strings

If one of the symmetries is broken by a single scalar at the high scale, and the other symmetry is broken by either one or two scalars at the low scale, then this can lead to a gravitational wave signature consisting of a phase transition bump over a cosmic string background. This signature was first proposed in [51] in the context of a different gauged baryon and lepton number model with a well-motivated large hierarchy between symmetry breaking scales, and recently considered in another scenario [160]. In Fig. 10 we show an example of such a signal, where $U(1)_L$ is broken at the scale $v_L = 10^6$ PeV, whereas the scale of $U(1)_B$ breaking is $v_B = 200$ TeV. The other parameter values for this particular plot are $g_B = 0.25$ and $\lambda_B = 0.006$. As in the previous case, by changing the scale of $U(1)_B$ breaking the bump can shift and become searchable not only by Big
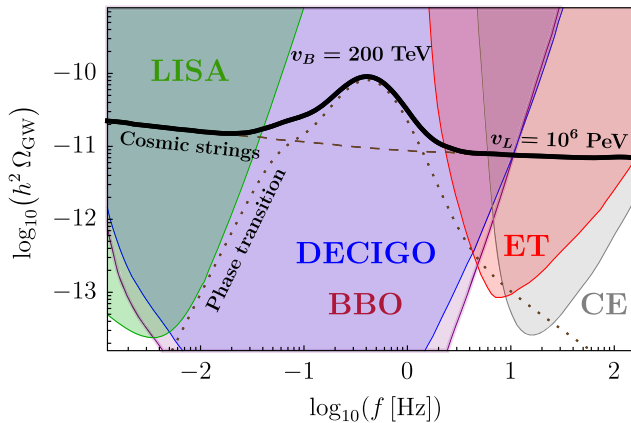

FIG. 10. Gravitational wave signature with a first order phase transition peak over a cosmic string background, first proposed in [51], realized when one U(1) is broken by only one scalar and the other U(1) is broken either by one or two scalars—models (a)–(c).
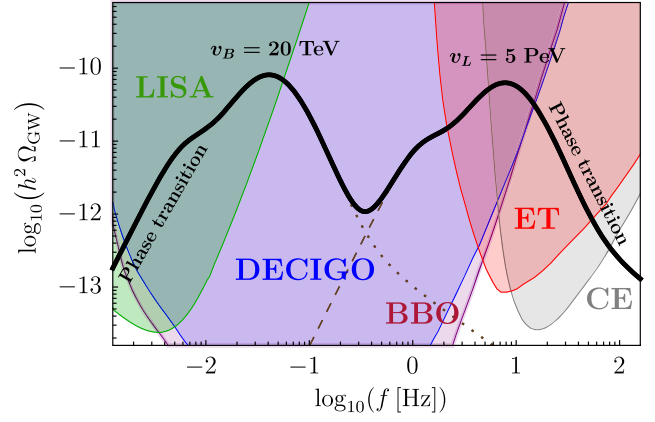

FIG. 11. Gravitational wave signature consisting of two first order phase transition peaks, similar to the ones proposed in [76,93,94], arising when the two U(1) symmetries are broken by any number of scalars—realized in models (a)–(d).

Bang Observer and DECIGO, but also by Cosmic Explorer, Einstein Telescope, or LISA.

D. Phase transition + phase transition

Independently of the scalar sector structure, the breaking of two U(1) gauge symmetries can always result in a gravitational wave signal with two first order phase transition peaks. Such a signature is generically expected in theories with a multistep symmetry breaking pattern, and has been proposed for various models of new physics [76,93,94]. In Fig. 11 a realization of this signature is shown in the case of our model, assuming that the $U(1)_B$ symmetry is broken by one scalar at the scale $v_B = 20$ TeV (the other parameters are $g_B = 0.25$ and $\lambda_B = 0.006$), and the $U(1)_L$ symmetry is broken also by one scalar at the scale $v_L = 5$ PeV (with $g_L = 0.20$ and $\lambda_L = 0.0025$). We note that for the two contributions appropriate formulas for the thermal masses were adopted, according to Eq. (39). Such a signal can be searched for in all the future gravitational wave detectors we considered.

E. Phase transition + domain walls

The final qualitatively different signature consists also of two peaks, but this time one coming from a first order phase transition and the second one arising from domain wall annihilation. Such a signal has very recently been proposed in [66]. In our model it can be realized if there is a large hierarchy between the $U(1)_B$ and $U(1)_L$ symmetry breaking scales. Figure 12 shows a realization of this scenario when $U(1)_L$ is broken by two scalars at the scale $v_L = 3 \times 10^4$ PeV (with a potential bias $\Delta\rho = 6.3 \times 10^3$ PeV^4), whereas $U(1)_B$ is broken by one scalar at the scale $v_B = 20$ TeV (with the other parameters being $g_B = 0.25$ and $\lambda_B = 0.006$). As pointed out in [66], the two peaks may appear in a different order, which would happen for a $U(1)_L$
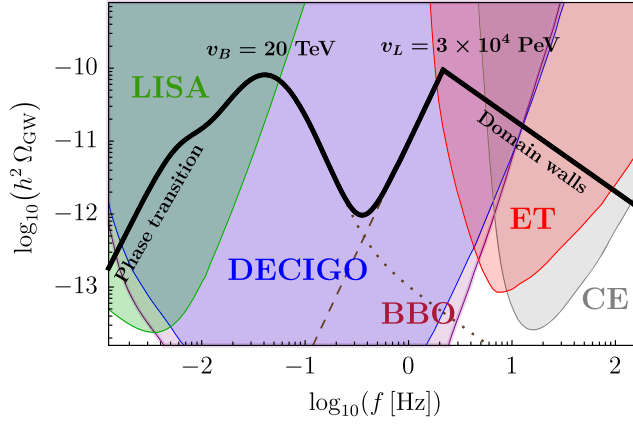
FIG. 12. Gravitational wave signature containing a phase transition peak and a domain wall peak, proposed in [66], realized when at least one U(1) symmetry is broken by two scalars—models (b)–(d).

breaking scale of $v_L \sim 10^3$ PeV and a U(1)$_B$ breaking scale of $v_B \sim 10$ PeV. In both scenarios, the signature can be searched for in the upcoming gravitational wave detectors we focused on.

Although the signatures discussed above can be realized for any pattern of symmetry breaking, the phenomenologically more attractive scenarios involve U(1)$_L$ broken at the high scale, so that the bound in Eq. (18) is satisfied and the theory can successfully accommodate leptogenesis, as discussed in Sec. III. Additionally, with no motivation for a low U(1)$_B$ breaking scale in the model we are considering, the new signatures shown in Figs. 8 and 9 can be naturally realized, and are quite appealing given the reach of the upcoming gravitational wave experiments.

VIII. CONCLUSIONS AND OUTLOOK

It is truly extraordinary that gravitational wave astronomy can join forces with elementary particle physics to search for answers to fundamental questions about the structure of the Universe and its earliest stages of evolution. Indeed, processes happening at energies too high to be probed by conventional particle physics detectors (such as high scale leptogenesis and seesaw mechanism) can leave a remarkable imprint through the primordial gravitational wave background emitted soon after the big bang. Detecting such a signal would bring us closer to discovering which, if any, of the proposed Standard Model extensions addressing the outstanding questions about dark matter, matter-antimatter asymmetry, or neutrino masses, is realized in nature.

A stochastic gravitational wave background is expected to originate in the early Universe within the framework of many particle physics models through first order phase transitions, cosmic string dynamics, and domain wall annihilation. In particular, explaining the matter-antimatter

asymmetry puzzle requires a first order phase transition to happen, indicating the huge importance of stochastic gravitational wave searches. The literature referred to in Sec. I contains analyses of such signatures in theories beyond the Standard Model; however, the majority of the works focus on one single component at a time, generally not looking at the possible interplay between the contributions from different sources.

In this paper we highlighted the importance of searches for novel gravitational wave signatures arising when multiple components are present in the spectrum and add up producing new features in the signal. Such unique signatures are expected in theories with more than one symmetry breaking, and result from the interplay between the contributions from first order phase transitions, cosmic strings, and/or domain walls. The new gravitational wave signals we propose to look for are these: (1) Double-sharp-peak structure from domain walls produced when two gauge symmetries are broken by multiple scalars; and (2) Domain wall peak over a cosmic string plateau when one symmetry is broken by a single scalar and the other symmetry is broken by multiple scalars.

Although we demonstrate how those signatures arise in a specific model with gauged baryon and lepton number, our results are applicable to a much wider class of theories with two U(1) gauge symmetries broken at different energy scales. Indeed, the new signals consist of the cosmic string and domain wall contributions, thus they are fairly model independent, since the cosmic string component depends only on the symmetry breaking scale, whereas the domain wall contribution depends on the symmetry breaking scale and the potential bias. Our results can also be extended to models with non-Abelian gauge groups. As already suggested in [66], it would be interesting to investigate the case when one of the symmetries is SU(2) broken by two scalar triplets, as this can result in the production of cosmic strings [161], and could perhaps lead to new signals involving contributions from all three processes: first order phase transitions, cosmic string dynamics, and domain wall annihilation.

The gravitational wave signatures discussed here can be searched for in upcoming experiments, including LISA, Big Bang Observer, DECIGO, Cosmic Explorer, and Einstein Telescope, enabling those detectors to probe the structure of high-scale symmetry breaking sectors. This is especially relevant for theories of leptogenesis such as the model we considered, in which, contrary to [19,51], the scale of U(1)$_B$ symmetry breaking is not bounded from above and can also be high, allowing for signals (1) and (2) to be generated.

Finally, it is worth mentioning that a spontaneous breaking of a single gauge symmetry can by itself lead to gravitational wave signatures combining signals from a phase transition and cosmic strings, or a phase transition and domain walls. Given the sensitivity of the experiments

considered, the symmetry breaking scale would have to be ~100–1000 PeV for the combined signal to be discoverable. The cosmic string contribution would then be detectable by Big Bang Observer and DECIGO, the phase transition peak could be seen by Cosmic Explorer and Einstein Telescope, and the domain wall peak would be visible in LISA. Investigating this in more detail is an interesting follow-up project, and could be tied to gravitational wave experiments sensitive to lower frequencies, such as the pulsar timing arrays: NANOGrav [162], PPTA [163], EPTA [164], IPTA [165], or SKA [166].

[1] S. L. Glashow, Partial symmetries of weak interactions, Nucl. Phys. **22**, 579 (1961).

[2] P. W. Higgs, Broken symmetries and the masses of gauge bosons, Phys. Rev. Lett. **13**, 508 (1964).

[3] F. Englert and R. Brout, Broken symmetry and the mass of gauge vector mesons, Phys. Rev. Lett. **13**, 321 (1964).

[4] S. Weinberg, A model of leptons, Phys. Rev. Lett. **19**, 1264 (1967).

[5] A. Salam, Weak and electromagnetic interactions, Conf. Proc. C **680519**, 367 (1968).

[6] H. Fritzsch, M. Gell-Mann, and H. Leutwyler, Advantages of the color octet gluon picture, Phys. Lett. **47B**, 365 (1973).

[7] D. J. Gross and F. Wilczek, Ultraviolet behavior of non-Abelian gauge theories, Phys. Rev. Lett. **30**, 1343 (1973).

[8] H. D. Politzer, Reliable perturbative results for strong interactions?, Phys. Rev. Lett. **30**, 1346 (1973).

[9] H. Georgi and S. L. Glashow, Unity of all elementary particle forces, Phys. Rev. Lett. **32**, 438 (1974).

[10] H. Fritzsch and P. Minkowski, Unified interactions of leptons and hadrons, Ann. Phys. (N.Y.) **93**, 193 (1975).

[11] K. Abe *et al.* (Super-Kamiokande Collaboration), Search for proton decay via $p \to e^+\pi^0$ and $p \to \mu^+\pi^0$ in 0.31 megaton · years exposure of the Super-Kamiokande water Cherenkov detector, Phys. Rev. D **95**, 012004 (2017).

[12] R. Kallosh, A. D. Linde, D. A. Linde, and L. Susskind, Gravity and global symmetries, Phys. Rev. D **52**, 912 (1995).

[13] A. Pais, Remark on baryon conservation, Phys. Rev. D **8**, 1844 (1973).

[14] S. Rajpoot, Gauge symmetries of electroweak interactions, Int. J. Theor. Phys. **27**, 689 (1988).

[15] R. Foot, G. C. Joshi, and H. Lew, Gauged baryon and lepton numbers, Phys. Rev. D **40**, 2487 (1989).

[16] C. D. Carone and H. Murayama, Realistic models with a light U(1) gauge boson coupled to baryon number, Phys. Rev. D **52**, 484 (1995).

[17] H. Georgi and S. L. Glashow, Decays of a leptophobic gauge boson, Phys. Lett. B **387**, 341 (1996).

[18] P. Fileviez Perez and M. B. Wise, Baryon and lepton number as local gauge symmetries, Phys. Rev. D **82**, 011901 (2010); **82**, 079901(E) (2010).

[19] M. Duerr, P. Fileviez Perez, and M. B. Wise, Gauge theory for baryon and lepton numbers with leptoquarks, Phys. Rev. Lett. **110**, 231801 (2013).

[20] P. Fileviez Perez, S. Ohmer, and H. H. Patel, Minimal theory for lepto-baryons, Phys. Lett. B **735**, 283 (2014).

[21] J. M. Arnold, P. Fileviez Perez, B. Fornal, and S. Spinner, B and L at the supersymmetry scale, dark matter, and R-parity violation, Phys. Rev. D **88**, 115009 (2013).

[22] B. Fornal, A. Rajaraman, and T. M. P. Tait, Baryon number as the fourth color, Phys. Rev. D **92**, 055022 (2015).

[23] B. Fornal and T. M. P. Tait, Dark matter from unification of color and baryon number, Phys. Rev. D **93**, 075010 (2016).

[24] B. Fornal, Y. Shirman, T. M. P. Tait, and J. Rittenhouse West, Asymmetric dark matter and baryogenesis from $SU(2)_\ell$, Phys. Rev. D **96**, 035001 (2017).

[25] M. Duerr and P. Fileviez Perez, Theory for baryon number and dark matter at the LHC, Phys. Rev. D **91**, 095001 (2015).

[26] S. Ohmer and H. H. Patel, Leptobaryons as Majorana dark matter, Phys. Rev. D **92**, 055020 (2015).

[27] P. Fileviez Perez, E. Golias, R.-H. Li, and C. Murgui, Leptophobic dark matter and the baryon number violation scale, Phys. Rev. D **99**, 035009 (2019).

[28] P. Fileviez Perez, C. Murgui, and A. D. Plascencia, Baryogenesis via leptogenesis: Spontaneous B and L violation, Phys. Rev. D **104**, 055007 (2021).

[29] B. P. Abbott *et al.* (LIGO Scientific and Virgo Collaborations), Observation of gravitational waves from a binary black hole merger, Phys. Rev. Lett. **116**, 061102 (2016).

[30] M. S. Turner, Detectability of inflation produced gravitational waves, Phys. Rev. D **55**, R435 (1997).

[31] A. Kosowsky, M. S. Turner, and R. Watkins, Gravitational radiation from colliding vacuum bubbles, Phys. Rev. D **45**, 4514 (1992).

[32] T. Hiramatsu, M. Kawasaki, and K. Saikawa, Gravitational waves from collapsing domain walls, J. Cosmol. Astropart. Phys. 05 (2010) 032.

[33] T. Vachaspati and A. Vilenkin, Gravitational radiation from cosmic strings, Phys. Rev. D **31**, 3052 (1985).

[34] M. Sakellariadou, Gravitational waves emitted from infinite strings, Phys. Rev. D **42**, 354 (1990); **43**, 4150(E) (1991).

[35] P. Amaro-Seoane *et al.* (LISA Collaboration), Laser interferometer space antenna, arXiv:1702.00786.

[36] D. Reitze *et al.*, Cosmic Explorer: The U.S. contribution to gravitational-wave astronomy beyond LIGO, Bull. Am. Astron. Soc. **51,** 035 (2019).

[37] M. Punturo *et al.*, The Einstein Telescope: A third-generation gravitational wave observatory, Classical Quantum Gravity **27,** 194002 (2010).

[38] S. Kawamura *et al.*, The Japanese space gravitational wave antenna: DECIGO, Classical Quantum Gravity **28,** 094011 (2011).

[39] J. Crowder and N. J. Cornish, Beyond LISA: Exploring future gravitational wave missions, Phys. Rev. D **72,** 083005 (2005).

[40] T. W. B. Kibble, Topology of cosmic domains and strings, J. Phys. A **9,** 1387 (1976).

[41] W. Buchmuller, V. Domcke, H. Murayama, and K. Schmitz, Probing the scale of grand unification with gravitational waves, Phys. Lett. B **809,** 135764 (2020).

[42] S. F. King, S. Pascoli, J. Turner, and Y.-L. Zhou, Gravitational waves and proton decay: Complementary windows into GUTs, Phys. Rev. Lett. **126,** 021802 (2021).

[43] J. J. Blanco-Pillado and K. D. Olum, Stochastic gravitational wave background from smoothed cosmic string loops, Phys. Rev. D **96,** 104046 (2017).

[44] C. Ringeval and T. Suyama, Stochastic gravitational waves from cosmic string loops in scaling, J. Cosmol. Astropart. Phys. 12 (2017) 027.

[45] Y. Cui, M. Lewicki, D. E. Morrissey, and J. D. Wells, Cosmic archaeology with gravitational waves from cosmic strings, Phys. Rev. D **97,** 123505 (2018).

[46] Y. Cui, M. Lewicki, D. E. Morrissey, and J. D. Wells, Probing the Pre-BBN universe with gravitational waves from cosmic strings, J. High Energy Phys. 01 (2019) 081.

[47] G. S. F. Guedes, P. P. Avelino, and L. Sousa, Signature of inflation in the stochastic gravitational wave background generated by cosmic string networks, Phys. Rev. D **98,** 123505 (2018).

[48] J. A. Dror, T. Hiramatsu, K. Kohri, H. Murayama, and G. White, Testing the seesaw mechanism and leptogenesis with gravitational waves, Phys. Rev. Lett. **124,** 041804 (2020).

[49] R. Zhou and L. Bian, Gravitational waves from cosmic strings and first-order phase transition, Chin. Phys. C **46,** 043104 (2022).

[50] Y. Gouttenoire, G. Servant, and P. Simakachorn, BSM with cosmic strings: Heavy, up to EeV mass, unstable particles, J. Cosmol. Astropart. Phys. 07 (2020) 016.

[51] B. Fornal and B. Shams Es Haghi, Baryon and lepton number violation from gravitational waves, Phys. Rev. D **102,** 115037 (2020).

[52] Y. Gouttenoire, G. Servant, and P. Simakachorn, Beyond the standard models with cosmic strings, J. Cosmol. Astropart. Phys. 07 (2020) 032.

[53] R. Abbott *et al.* (LIGO Scientific, Virgo, and KAGRA Collaborations), Constraints on cosmic strings using data from the third Advanced LIGO–Virgo observing run, Phys. Rev. Lett. **126,** 241102 (2021).

[54] M. Eto, M. Kurachi, and M. Nitta, Constraints on two Higgs doublet models from domain walls, Phys. Lett. B **785,** 447 (2018).

[55] M. Eto, M. Kurachi, and M. Nitta, Non-Abelian strings and domain walls in two Higgs doublet models, J. High Energy Phys. 08 (2018) 195.

[56] N. Chen, T. Li, Z. Teng, and Y. Wu, Collapsing domain walls in the two-Higgs-doublet model and deep insights from the EDM, J. High Energy Phys. 10 (2020) 081.

[57] R. A. Battye, A. Pilaftsis, and D. G. Viatic, Domain wall constraints on two-Higgs-doublet models with Z_2 symmetry, Phys. Rev. D **102,** 123536 (2020).

[58] K. Kadota, M. Kawasaki, and K. Saikawa, Gravitational waves from domain walls in the next-to-minimal supersymmetric standard model, J. Cosmol. Astropart. Phys. 10 (2015) 041.

[59] N. Craig, I. Garcia Garcia, G. Koszegi, and A. McCune, P not PQ, J. High Energy Phys. 09 (2021) 130.

[60] G. B. Gelmini, A. Simpson, and E. Vitagliano, Gravitational waves from axionlike particle cosmic string-wall networks, Phys. Rev. D **104,** L061301 (2021).

[61] R. Z. Ferreira, A. Notari, O. Pujolas, and F. Rompineve, High quality QCD axion at gravitational wave observatories, Phys. Rev. Lett. **128,** 141101 (2022).

[62] G. B. Gelmini, A. Simpson, and E. Vitagliano, Catastrogenesis: DM, GWs, and PBHs from ALP string-wall networks, J. Cosmol. Astropart. Phys. 02 (2023) 031.

[63] S. Blasi, A. Mariotti, A. Rase, A. Sevrin, and K. Turbang, Friction on ALP domain walls and gravitational waves, J. Cosmol. Astropart. Phys. 04 (2023) 008.

[64] D. I. Dunsky, A. Ghoshal, H. Murayama, Y. Sakakihara, and G. White, GUTs, hybrid topological defects, and gravitational waves, Phys. Rev. D **106,** 075030 (2022).

[65] D. Borah and A. Dasgupta, Probing left-right symmetry via gravitational waves from domain walls, Phys. Rev. D **106,** 035016 (2022).

[66] B. Fornal, K. Garcia, and E. Pierre, Testing unification and dark matter with gravitational waves, Phys. Rev. D **108,** 055022 (2023).

[67] G. B. Gelmini, S. Pascoli, E. Vitagliano, and Y.-L. Zhou, Gravitational wave signatures from discrete flavor symmetries, J. Cosmol. Astropart. Phys. 02 (2021) 032.

[68] B. Barman, D. Borah, A. Dasgupta, and A. Ghoshal, Probing high scale Dirac leptogenesis via gravitational waves from domain walls, Phys. Rev. D **106,** 015007 (2022).

[69] K. Saikawa, A review of gravitational waves from cosmic domain walls, Universe **3,** 40 (2017).

[70] Y. Jiang and Q.-G. Huang, Implications for cosmic domain walls from the first three observing runs of LIGO-Virgo, Phys. Rev. D **106,** 103036 (2022).

[71] C. Grojean and G. Servant, Gravitational waves from phase transitions at the electroweak scale and beyond, Phys. Rev. D **75,** 043507 (2007).

[72] V. Vaskonen, Electroweak baryogenesis and gravitational waves from a real scalar singlet, Phys. Rev. D **95,** 123515 (2017).

[73] G. C. Dorsch, S. J. Huber, T. Konstandin, and J. M. No, A second Higgs doublet in the early universe: Baryogenesis and gravitational waves, J. Cosmol. Astropart. Phys. 05 (2017) 052.

[74] J. Bernon, L. Bian, and Y. Jiang, A new insight into the phase transition in the early universe with two Higgs doublets, J. High Energy Phys. 05 (2018) 151.

[75] M. Chala, C. Krause, and G. Nardini, Signals of the electroweak phase transition at colliders and gravitational wave observatories, J. High Energy Phys. 07 (2018) 062.

[76] A. Angelescu and P. Huang, Multistep strongly first order phase transitions from new fermions at the TeV scale, Phys. Rev. D **99,** 055023 (2019).

[77] A. Alves, T. Ghosh, H.-K. Guo, K. Sinha, and D. Vagie, Collider and gravitational wave complementarity in exploring the singlet extension of the standard model, J. High Energy Phys. 04 (2019) 052.

[78] X.-F. Han, L. Wang, and Y. Zhang, Dark matter, electroweak phase transition, and gravitational waves in the type II two-Higgs-doublet model with a singlet scalar field, Phys. Rev. D **103,** 035012 (2021).

[79] N. Benincasa, L. Delle Rose, K. Kannike, and L. Marzola, Multistep phase transitions and gravitational waves in the inert doublet model, J. Cosmol. Astropart. Phys. 12 (2022) 025.

[80] N. Craig, N. Levi, A. Mariotti, and D. Redigolo, Ripples in spacetime from broken supersymmetry, J. High Energy Phys. 02 (2020) 184.

[81] B. Fornal, B. Shams Es Haghi, J.-H. Yu, and Y. Zhao, Gravitational waves from mini-split SUSY, Phys. Rev. D **104,** 115005 (2021).

[82] P. S. B. Dev, F. Ferrer, Y. Zhang, and Y. Zhang, Gravitational waves from first-order phase transition in a simple axion-like particle model, J. Cosmol. Astropart. Phys. 11 (2019) 006.

[83] B. Von Harling, A. Pomarol, O. Pujolas, and F. Rompineve, Peccei-Quinn phase transition at LIGO, J. High Energy Phys. 04 (2020) 195.

[84] L. Delle Rose, G. Panico, M. Redi, and A. Tesi, Gravitational waves from supercool axions, J. High Energy Phys. 04 (2020) 025.

[85] D. Croon, T. E. Gonzalo, and G. White, Gravitational waves from a Pati-Salam phase transition, J. High Energy Phys. 02 (2019) 083.

[86] W.-C. Huang, F. Sannino, and Z.-W. Wang, Gravitational waves from Pati-Salam dynamics, Phys. Rev. D **102,** 095025 (2020).

[87] N. Okada, O. Seto, and H. Uchida, Gravitational waves from breaking of an extra $U(1)$ in $SO(10)$ grand unification, Prog. Theor. Exp. Phys. **2021,** 033B01 (2021).

[88] T. Hasegawa, N. Okada, and O. Seto, Gravitational waves from the minimal gauged $U(1)_{B-L}$ model, Phys. Rev. D **99,** 095039 (2019).

[89] V. Brdar, A. J. Helmboldt, and J. Kubo, Gravitational waves from first-order phase transitions: LIGO as a window to unexplored seesaw scales, J. Cosmol. Astropart. Phys. 02 (2019) 021.

[90] N. Okada and O. Seto, Probing the seesaw scale with gravitational waves, Phys. Rev. D **98,** 063532 (2018).

[91] P. Di Bari, D. Marfatia, and Y.-L. Zhou, Gravitational waves from first-order phase transitions in Majoron models of neutrino mass, J. High Energy Phys. 10 (2021) 193.

[92] R. Zhou, L. Bian, and Y. Du, Electroweak phase transition and gravitational waves in the type-II seesaw model, J. High Energy Phys. 08 (2022) 205.

[93] A. Greljo, T. Opferkuch, and B. A. Stefanek, Gravitational imprints of flavor hierarchies, Phys. Rev. Lett. **124,** 171802 (2020).

[94] B. Fornal, Gravitational wave signatures of lepton universality violation, Phys. Rev. D **103,** 015018 (2021).

[95] P. Schwaller, Gravitational waves from a dark phase transition, Phys. Rev. Lett. **115,** 181101 (2015).

[96] M. Breitbach, J. Kopp, E. Madge, T. Opferkuch, and P. Schwaller, Dark, cold, and noisy: Constraining secluded hidden sectors with gravitational waves, J. Cosmol. Astropart. Phys. 07 (2019) 007.

[97] D. Croon, V. Sanz, and G. White, Model discrimination in gravitational wave spectra from dark phase transitions, J. High Energy Phys. 08 (2018) 203.

[98] E. Hall, T. Konstandin, R. McGehee, H. Murayama, and G. Servant, Baryogenesis from a dark first-order phase transition, J. High Energy Phys. 04 (2020) 042.

[99] J. Ellis, M. Lewicki, and V. Vaskonen, Updated predictions for gravitational waves produced in a strongly supercooled phase transition, J. Cosmol. Astropart. Phys. 11 (2020) 020.

[100] K. Kawana, Cosmology of a supercooled universe, Phys. Rev. D **105,** 103515 (2022).

[101] I. Baldes, Gravitational waves from the asymmetric-dark-matter generating phase transition, J. Cosmol. Astropart. Phys. 05 (2017) 028.

[102] A. Azatov, M. Vanvlasselaer, and W. Yin, Dark matter production from relativistic bubble walls, J. High Energy Phys. 03 (2021) 288.

[103] F. Costa, S. Khan, and J. Kim, A two-component dark matter model and its associated gravitational waves, J. High Energy Phys. 06 (2022) 026.

[104] F. Costa, S. Khan, and J. Kim, A two-component vector WIMP—Fermion FIMP dark matter model with an extended seesaw mechanism, J. High Energy Phys. 12 (2022) 165.

[105] B. Fornal and E. Pierre, Asymmetric dark matter from gravitational waves, Phys. Rev. D **106,** 115040 (2022).

[106] M. Kierkla, A. Karam, and B. Swiezewska, Conformal model for gravitational waves and dark matter: A status update, J. High Energy Phys. 03 (2023) 007.

[107] A. Azatov, G. Barni, S. Chakraborty, M. Vanvlasselaer, and W. Yin, Ultra-relativistic bubbles from the simplest Higgs portal and their cosmological consequences, J. High Energy Phys. 10 (2022) 017.

[108] R. Caldwell *et al.*, Detection of early-universe gravitational-wave signatures and fundamental physics, Gen. Relativ. Gravit. **54,** 156 (2022).

[109] P. Athron, C. Balazs, A. Fowlie, L. Morris, and L. Wu, Cosmological phase transitions: From perturbative particle physics to gravitational waves, arXiv:2305.02357.

[110] C. Badger, B. Fornal, K. Martinovic, A. Romero, K. Turbang, H. Guo, A. Mariotti, M. Sakellariadou, A. Sevrin, F.-W. Yang, and Y. Zhao, Probing early universe supercooled phase transitions with gravitational wave data, Phys. Rev. D **107,** 023511 (2023).

[111] J. Ellis, M. Lewicki, J. M. No, and V. Vaskonen, Gravitational wave energy budget in strongly supercooled phase transitions, J. Cosmol. Astropart. Phys. 06 (2019) 024.

[112] M. Lewicki and V. Vaskonen, On bubble collisions in strongly supercooled phase transitions, Phys. Dark Universe **30**, 100672 (2020).

[113] M. Lewicki and V. Vaskonen, Gravitational wave spectra from strongly supercooled phase transitions, Eur. Phys. J. C **80**, 1003 (2020).

[114] N. Aghanim *et al.* (Planck Collaboration), Planck 2018 results. VI. Cosmological parameters, Astron. Astrophys. **641**, A6 (2020); **652**, C4(E) (2021).

[115] S. Davidson, E. Nardi, and Y. Nir, Leptogenesis, Phys. Rep. **466**, 105 (2008).

[116] W. Buchmuller, P. Di Bari, and M. Plumacher, Leptogenesis for pedestrians, Ann. Phys. (Amsterdam) **315**, 305 (2005).

[117] R. L. Workman *et al.* (Particle Data Group), Review of particle physics, Prog. Theor. Exp. Phys. **2022**, 083C01 (2022).

[118] A. Vilenkin and E. P. S. Shellard, *Cosmic Strings and Other Topological Defects* (Cambridge University Press, Cambridge, England, 2000).

[119] P. A. R. Ade *et al.* (Planck Collaboration), Planck 2013 Results. XXV. Searches for cosmic strings and other topological defects, Astron. Astrophys. **571**, A25 (2014).

[120] K. D. Olum and J. J. Blanco-Pillado, Radiation from cosmic string standing waves, Phys. Rev. Lett. **84**, 4288 (2000).

[121] J. N. Moore, E. P. S. Shellard, and C. J. A. P. Martins, On the evolution of Abelian-Higgs string networks, Phys. Rev. D **65**, 023503 (2002).

[122] T. W. B. Kibble, Evolution of a system of cosmic strings, Nucl. Phys. **B252**, 227 (1985); **B261**, 750(E) (1985).

[123] D. P. Bennett and F. R. Bouchet, Evidence for a scaling solution in cosmic-string evolution, Phys. Rev. Lett. **60**, 257 (1988).

[124] D. P. Bennett and F. R. Bouchet, Cosmic-string evolution, Phys. Rev. Lett. **63**, 2776 (1989).

[125] A. Albrecht and N. Turok, Evolution of cosmic string networks, Phys. Rev. D **40**, 973 (1989).

[126] B. Allen and E. P. S. Shellard, Cosmic-string evolution: A numerical simulation, Phys. Rev. Lett. **64**, 119 (1990).

[127] M. B. Hindmarsh and T. W. B. Kibble, Cosmic strings, Rep. Prog. Phys. **58**, 477 (1995).

[128] J. J. Blanco-Pillado, K. D. Olum, and B. Shlaer, The number of cosmic string loops, Phys. Rev. D **89**, 023512 (2014).

[129] T. Vachaspati and A. Vilenkin, Gravitational radiation from cosmic strings, Phys. Rev. D **31**, 3052 (1985).

[130] C. J. A. P. Martins and E. P. S. Shellard, String evolution with friction, Phys. Rev. D **53**, R575 (1996).

[131] C. J. A. P. Martins and E. P. S. Shellard, Quantitative string evolution, Phys. Rev. D **54**, 2535 (1996).

[132] C. J. A. P. Martins and E. P. S. Shellard, Extending the velocity dependent one scale string evolution model, Phys. Rev. D **65**, 043514 (2002).

[133] D. Matsunami, L. Pogosian, A. Saurabh, and T. Vachaspati, Decay of cosmic string loops due to particle radiation, Phys. Rev. Lett. **122**, 201301 (2019).

[134] M. Hindmarsh, J. Lizarraga, A. Urio, and J. Urrestilla, Loop decay in Abelian-Higgs string networks, Phys. Rev. D **104**, 043519 (2021).

[135] J. J. Blanco-Pillado, D. Jimenez-Aguilar, J. Lizarraga, A. Lopez-Eiguren, K. D. Olum, A. Urio, and J. Urrestilla, Nambu-Goto dynamics of field theory cosmic string loops, J. Cosmol. Astropart. Phys. 05 (2023) 035.

[136] I. F. Ginzburg and M. Krawczyk, Symmetries of two Higgs doublet model and *CP* violation, Phys. Rev. D **72**, 115013 (2005).

[137] R. A. Battye, G. D. Brawn, and A. Pilaftsis, Vacuum topology of the two Higgs doublet model, J. High Energy Phys. 08 (2011) 020.

[138] G. C. Branco, P. M. Ferreira, L. Lavoura, M. N. Rebelo, M. Sher, and J. P. Silva, Theory and phenomenology of two-Higgs-doublet models, Phys. Rep. **516**, 1 (2012).

[139] T. Hiramatsu, M. Kawasaki, and K. Saikawa, On the estimation of gravitational wave spectrum from cosmic domain walls, J. Cosmol. Astropart. Phys. 02 (2014) 031.

[140] R. Z. Ferreira, A. Notari, O. Pujolas, and F. Rompineve, Gravitational waves from domain walls in pulsar timing array datasets, J. Cosmol. Astropart. Phys. 02 (2023) 001.

[141] A. Afzal *et al.* (NANOGrav Collaboration), The NANO-Grav 15 yr data set: Search for signals from new physics, Astrophys. J. Lett. **951**, L11 (2023).

[142] T. J. Clarke, E. J. Copeland, and A. Moss, Constraints on primordial gravitational waves from the cosmic microwave background, J. Cosmol. Astropart. Phys. 10 (2020) 002.

[143] D. Croon, O. Gould, P. Schicho, T. V. I. Tenkanen, and G. White, Theoretical uncertainties for cosmological first-order phase transitions, J. High Energy Phys. 04 (2021) 055.

[144] P. Athron, C. Balazs, A. Fowlie, L. Morris, G. White, and Y. Zhang, How arbitrary are perturbative calculations of the electroweak phase transition?, J. High Energy Phys. 01 (2023) 050.

[145] A. D. Linde, Decay of the false vacuum at finite temperature, Nucl. Phys. **B216**, 421 (1983).

[146] J. R. Espinosa, T. Konstandin, J. M. No, and G. Servant, Energy budget of cosmological first-order phase transitions, J. Cosmol. Astropart. Phys. 06 (2010) 028.

[147] C. Caprini *et al.*, Science with the space-based interferometer eLISA. II: Gravitational waves from cosmological phase transitions, J. Cosmol. Astropart. Phys. 04 (2016) 001.

[148] M. Hindmarsh, S. J. Huber, K. Rummukainen, and D. J. Weir, Gravitational waves from the sound of a first order phase transition, Phys. Rev. Lett. **112**, 041301 (2014).

[149] J. Ellis, M. Lewicki, and J. M. No, Gravitational waves from first-order cosmological phase transitions: Lifetime of the sound wave source, J. Cosmol. Astropart. Phys. 07 (2020) 050.

[150] H.-K. Guo, K. Sinha, D. Vagie, and G. White, Phase transitions in an expanding universe: Stochastic gravitational waves in standard and non-standard histories, J. Cosmol. Astropart. Phys. 01 (2021) 001.

[151] S. J. Huber and T. Konstandin, Gravitational wave production by collisions: More bubbles, J. Cosmol. Astropart. Phys. 09 (2008) 022.

[152] M. Lewicki and V. Vaskonen, Gravitational waves from colliding vacuum bubbles in gauge theories, Eur. Phys. J. C **81**, 437 (2021).

[153] M. Kamionkowski, A. Kosowsky, and M. S. Turner, Gravitational radiation from first order phase transitions, Phys. Rev. D **49,** 2837 (1994).

[154] C. Caprini and R. Durrer, Gravitational waves from stochastic relativistic sources: Primordial turbulence and magnetic fields, Phys. Rev. D **74,** 063521 (2006).

[155] C. Caprini, R. Durrer, and G. Servant, The stochastic gravitational wave background from turbulence and magnetic fields generated by a first-order phase transition, J. Cosmol. Astropart. Phys. 12 (2009) 024.

[156] D. Cutting, M. Hindmarsh, and D. J. Weir, Vorticity, kinetic energy, and suppressed gravitational wave production in strong first order phase transitions, Phys. Rev. Lett. **125,** 021302 (2020).

[157] R.-G. Cai, S.-J. Wang, and Z.-Y. Yuwen, Hydrodynamic sound shell model, Phys. Rev. D **108,** L021502 (2023).

[158] M. Hindmarsh and M. Hijazi, Gravitational waves from first order cosmological phase transitions in the sound shell model, J. Cosmol. Astropart. Phys. 12 (2019) 062.

[159] C. Gowling and M. Hindmarsh, Observational prospects for phase transitions at LISA: Fisher matrix analysis, J. Cosmol. Astropart. Phys. 10 (2021) 039.

[160] F. Ferrer, A. Ghoshal, and M. Lewicki, Imprints of a supercooled universe in the gravitational wave spectrum from a cosmic string network, J. High Energy Phys. 09 (2023) 036.

[161] M. Hindmarsh, K. Rummukainen, and D. J. Weir, New solutions for non-Abelian cosmic strings, Phys. Rev. Lett. **117,** 251601 (2016).

[162] Z. Arzoumanian *et al.* (NANOGRAV Collaboration), The NANOGrav 11-year data set: Pulsar-timing constraints on the stochastic gravitational-wave background, Astrophys. J. **859,** 47 (2018).

[163] R. N. Manchester *et al.*, The Parkes pulsar timing array project, Publ. Astron. Soc. Aust. **30,** e017 (2013).

[164] R. D. Ferdman *et al.*, The European pulsar timing array: Current efforts and a LEAP toward the future, Classical Quantum Gravity **27,** 084014 (2010).

[165] G. Hobbs *et al.*, The international pulsar timing array project: Using pulsars as a gravitational wave detector, Classical Quantum Gravity **27,** 084013 (2010).

[166] A. Weltman *et al.*, Fundamental physics with the square kilometre array, Publ. Astron. Soc. Aust. **37,** e002 (2020).